



FBG_SiMul V1.0: Fibre Bragg grating signal simulation tool for finite element method models

G. Pereira^{*}, M. McGugan, L.P. Mikkelsen

Technical University of Denmark, Department of Wind Energy, Frederiksborgvej 399, 4000 Roskilde, Denmark

Received 23 March 2016; received in revised form 25 July 2016; accepted 23 August 2016

Abstract

FBG_SiMul V1.0 is a tool to study and design the implementation of fibre Bragg grating (FBG) sensors solutions in any arbitrary loaded structure or application. The software removes the need for a fibre optic expert user and makes the sensor response of a structural health monitoring solution using FBG sensors more simple and fast. The software uses a modified *T*-Matrix method to simulate the FBG reflected spectrum based on the stress and strain from a finite element method model. The article describes the theory and algorithm implementation, followed by an empirical validation.

© 2016 The Author(s). Published by Elsevier B.V. This is an open access article under the CC BY license (<http://creativecommons.org/licenses/by/4.0/>).

Keywords: Fibre Bragg grating; FBG output simulation; FBG sensing solution design; FBG implementation; FBG optimization

Code metadata

Current software version	V1.0
Permanent link to executables of this version	https://github.com/ElsevierSoftwareX/SOFTX-D-16-00034
Legal Software License	GNU GPL-3
Computing platform/ Operating System	Windows;
Installation requirements & dependencies	None for standalone file; Python 2.7.5 for Python format;
If available, link to user manual - if formally published include a reference to the publication in the reference list	https://github.com/GilmarPereira/FBG_SiMul/blob/master/Standalone_Version/Software_Documentation.pdf
Support email for questions	gfpe@dtu.dk ; gilmar_fp@outlook.com ;

1. Introduction

More demanding structural applications and new design philosophies are increasingly motivating engineers and researchers to implement sensors into structures and to develop new structural health monitoring (SHM) solutions [1,2]. This opportunity is driven by new low-cost sensors and transducers, new electronics and new manufacturing techniques. In particular, the cost of fibre Bragg grating (FBG) sensors has dropped

over the last few years and robust fibre-optic monitoring systems suitable for SHM have become commercial off the shelf hardware.

However, the sustainment of structures using these permanent on-board health monitoring systems is a complex and multi-disciplinary technological field that requires a holistic approach that cannot be addressed solely by advances in the various technology platforms on which the SHM is constructed. What is required is twofold; that the next generation of research scientists and engineers are specifically trained with the skills, research experience, and multi-disciplinary background to adopt the new structural sustainment concepts. And that tools are available that enable the demanding task of integrating,

^{*} Corresponding author.

E-mail address: gfpe@dtu.dk (G. Pereira).

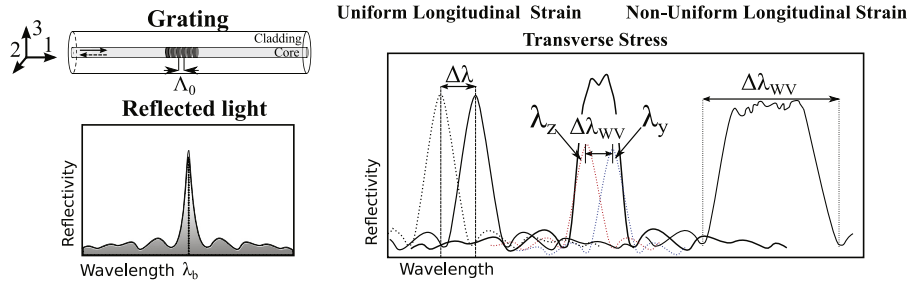


Fig. 1. Fibre Bragg grating response for uniform strain, transverse stress and non-uniform strain.

supporting, and maintaining an innovative holistic health management system and to propel its application in the aerospace, wind energy, and other industries.

The FBG_SiMul software described here is an example of the type of tool that will allow sensor simulation to become part of the design process, where output is simulated and optimized to a structure. This will have an immediate impact on the planning, development and implementation of SHM as well as provoking further research and development to include active control elements in the software and real-time data-driven feedback control for smart structures in the future. Equally important is that the software is robust and runs from a user-friendly interface. This ensures its uptake both within and outside the modelling and sensor communities, as it provides an opportunity for non-experts to simulate the signals and support their sensor implementation plans; whether for a one-off full-scale structural test, or a series of mechanical test specimens [3].

2. Problems and background

The shape and response of the FBG reflected spectrum (measured signal) depends on the way that the grating is deformed, i.e., the stress and strain field acting along the grating define the signal response. The FBG response simulation based on the stress and strain state from a finite element method (FEM) model was only recently addressed. *Hu et al.* [4] developed a Matlab code to simulate the FBG response under non-uniform strain fields caused by the transverse cracking in cross-ply laminates; and in a similar work, *Hasoon et al.* [5] developed a Matlab code to simulate the FBG response for mode-I delamination detection. However, the code developed by both authors is limited either by the type of FEM model or by the type of sensor response analysed; and, in both cases, the code/algorithm for the signal simulation code is not provided. Thus, FBG_SiMul was developed to tackle this gap in the FBG simulation field, where the FBG response is simulated independently of the structure, loading, or type of application. This because the software removes the need for a fibre optic expert user, making the FBG sensor response of a structural health monitoring solution becomes more intuitive and fast.

In the next section, it is presented the sensor working principle and the top level structure of the algorithm implemented in the software. For detailed information about the different theory used and the structure of the algorithm implemented see [Appendices A](#) and [B](#).

2.1. Fibre Bragg grating signal response

A FBG sensor is formed by a permanent periodic modulation of the refractive index along its core. When the optical fibre is illuminated by a broadband light source a narrow wavelength band is reflected back [3], as shown in [Fig. 1](#). The parameter Λ_0 represents the grating nominal period in an unstrained state, and λ_b is the wavelength of the reflected peak.

Any external force acting in the grating region changes the effective index and/or the period of modulation, which creates a shift in the wavelength and can modify the shape of the reflected peak. However, different stress and strain fields acting in the FBG sensor create different signal responses [3,11–14] (see [Fig. 1](#)); a longitudinal uniform strain field creates a wavelength shift in the reflected peak ($\Delta\lambda$), but the reflected peak shape remains unchanged; a longitudinal uniform and non-uniform strain field, acting along the grating, causes an increase in the reflected peak width ($\Delta\lambda_{WV}$) and a wavelength shift ($\Delta\lambda$); a transverse stress field, acting along the grating, causes a separation of the reflected Bragg peak due to the optical fibre birefringent behaviour, which can be described by an increase in the reflected peak width ($\Delta\lambda_{WV}$) and a wavelength shift ($\Delta\lambda$).

2.2. Spectrum simulation: transfer-matrix method

The transfer-matrix method was originally developed to simulate the reflected spectrum of FBG sensors under a uniform strain field by *Yamada and Sakuda* [6]; later, this theory was modified to simulate the reflected spectrum of FBG sensors under other types of strain field or different FBG configurations [7–10]. The modified *T*-Matrix method, developed by *Peters et al.* [7], consists of dividing the waveguides (grating periodic pattern) into short segments, where in each grating segment is assumed to be periodic. This assumption allows each segment to be handled as a uniform grating and its signal to be simulated by the original *Yamada T*-Matrix method. Then, when the grating is deformed, the grating period (Λ) in each segment is calculated using the average strain acting in that location; and, the total reflected signal is reconstructed by combining the signal contribution from all segments.

2.3. From a Finite Element Method model to spectrum simulation

In a FEM model the structure domain is divided in small sections called elements, which contain stress and strain

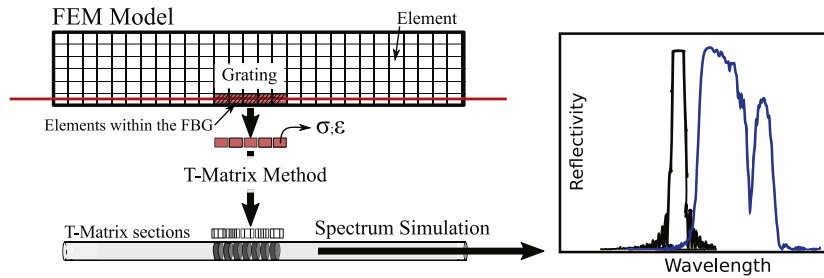


Fig. 2. Schematic representation of the algorithm implemented in the FBG_SiMul software: from a finite element method model to fibre Bragg grating spectrum simulation.

(among other information) used to describe the structure mechanical behaviour. In the *T*-Matrix method the grating is divided into short segments, and the simulated signal from each segment is added to the total reflected signal. Thus, it is possible to simulate the FBG reflected spectrum based on a FEM model, by matching the number of short segments used by the *T*-Matrix method with the number of elements in the FEM model, as shown in Fig. 2.

Then, the stress and strain from each FEM element is used by FBG_SiMul to simulate the sensor signal, using a modified *T*-Matrix method. The different theories implemented in FBG_SiMul algorithm are described in Appendices A and B.

3. Software description

FBG_SiMul was developed with a graphical user-interface, and no programming knowledge is required to perform FBG simulation; all the input parameters are pre-checked by the software, meaning that the simulation is robust and the code does not crash. The source code (python) is provided and it can be re-used or changed to fit any purpose.

The software is provided in two formats: a standalone file, in .exe format, which does not require installation or any dedicated software; and, in Python format, which can be modified but requires a python compiler. A user manual is provided together with the software, where the user can find information about the code structure, the type of functions/algorithms implemented, the software input/output and different functionalities, and a software tutorial case.

3.1. Software conceptual structure

The FBG_SiMul conceptual structure is shown in Fig. 3. First, the software extracts the stress and strain along a predefined path in a FEM model and save it as a .txt file. This can be made for a specific/single time increment, or for multiple time increments (useful for dynamic and time-dependent behaviour models). Next, the software identifies the FEM elements that lay inside of each FBG, and creates a local variable, per FBG sensor, containing all information needed to simulate the FBG response, as such as the number of elements per grating and the stress/strain field. Finally, two simulation options are given to the user: reflected spectrum simulation for a specific time increment, which allows evaluating the shape of the reflected signal; and, FBG time response, which simulates the sensor response for multiple time increments.

3.2. Software functionalities

The software is divided between 4 tabs according to functionalities:

- **Tab 1—Software:** Software front page, where the user can find information about all the different tabs and their functionalities, open the user manual, or learn more about the software copyright and author;
- **Tab 2—Extract Stress/Strain along Optical Fibre (Abaqus):** Tool to automatically extract the stress and strain along a pre-defined path in a *Abaqus* FEM model. The output is a .txt file containing the stress and strain distribution along a FBG path for a specific time increment. Tool options: multiple FBG paths; coordinate system rotation; single or multiple time increment;

Note: this tool was developed for *Abaqus* FEM models. Nevertheless, the user can simulate the FBG response using a different FEM software by extracting the files manually, and ensuring that the files have the required format, as described in the user manual.

- **Tab 3—FBG Spectrum Simulation (Specific Step Increment):** FBG reflected spectrum simulation for a specific time increment. Here, the user can study the FBG spectrum response, plan the sensor location, optimize the sensor wavelength, check available bandwidth, evaluate signal distortion or measurement errors, and so forth. The tab output is the FBG reflected spectrum, and it can be saved as an image or as a .txt file. Tool options: different SI units, mm or m; type of simulation, as longitudinal uniform strain, longitudinal non-uniform strain or transverse stress; user-defined optical fibre parameters; number of FBG sensors per fibre; FBG length; user-defined FBG array configuration; plot configuration.
- **Tab 4—FBG Signal variation (Time Response):** FBG signal response for multiple time increments. In this tab, the user can study the wavelength shift variation ($\Delta\lambda_{wv}$) and the peak width variation ($\Delta\lambda$) along the selected time increments, compare the sensor response for multiple FBG paths, plan the sensor location, and so forth. The tab output is the $\Delta\lambda_{wv}$ and $\Delta\lambda$ along the selected time increments, and it can be saved as an image or as a .txt file. Tool options: different SI units, mm or m; user-defined optical fibre parameters; number of FBG sensors per fibre; FBG length; user-defined FBG array configuration; plot configuration;

FBG_SiMul Conceptual Structure

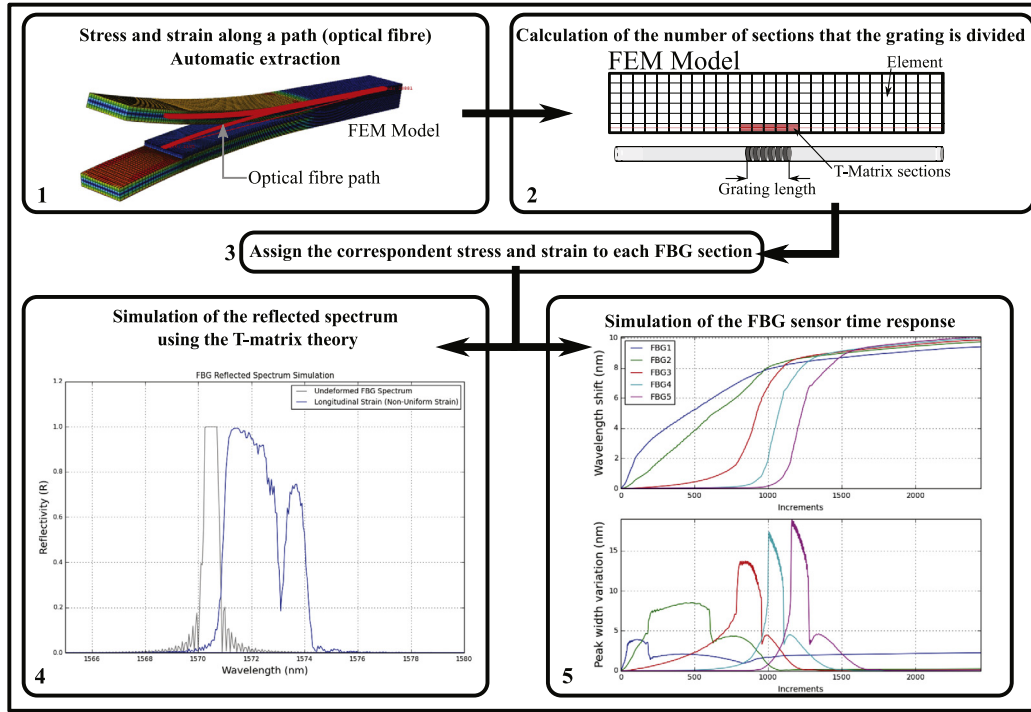


Fig. 3. FBG_SiMul conceptual structure. Fibre Bragg grating spectrum simulation from a finite element method.

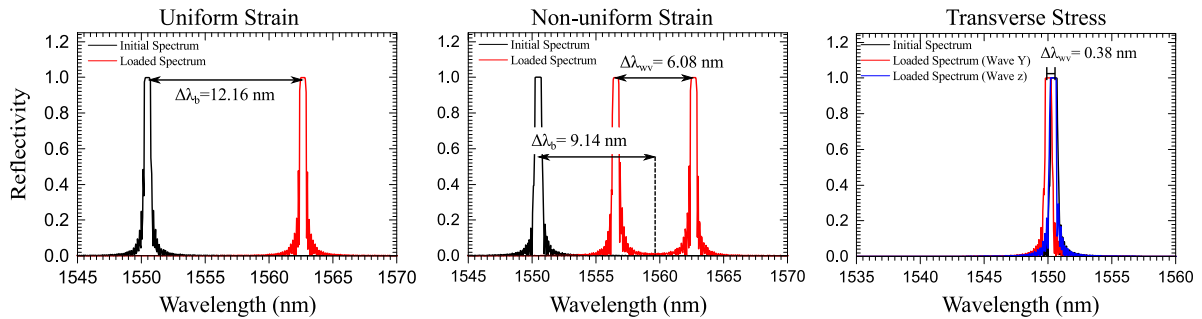


Fig. 4. FBG_SiMul simulation of the theoretical benchmark cases: The black lines represent the unloaded reflected spectrum, and the red (blue) line represent the deformed reflected spectrum. (For interpretation of the references to colour in this figure legend, the reader is referred to the web version of this article.)

4. Software empirical validation

To validate the software algorithm, 3 input files representing known cases of uniform strain, non-uniform strain and transverse stress were created. Each input file contains the stress and strain along a 10 mm grating, discretized in 20 segments. The theoretical wavelength shift, $\Delta\lambda_{wv}$, and theoretical peak width variation, $\Delta\lambda$, for the 3 cases were calculated using the analytical equations (3), (7), and (11) developed by Pereira et al. [3]. The analytical equations were solved using the following default parameters: photo-elastic coefficient $p_e = 0.215$; wavelength of the reflected peak $\lambda_b = 1550$ nm; refractive index $n_{eff} = 1.46$; grating nominal period $\Lambda_0 = 530.82$; direction dependent photo-elastic coefficient $p_{11} = 0.121$, $p_{12} = 0.270$; optical fibre elastic modulus $E = 70$ GPa; optical fibre Poisson's ratio $\nu = 0.17$.

Theoretical Benchmark cases:

- Uniform strain: grating under 1.0 $\varepsilon(\%)$ longitudinal strain.

- Non-uniform strain: half grating under 1.0 $\varepsilon(\%)$ and the other half under 0.5 $\varepsilon(\%)$ longitudinal strain.
- Transverse stress: grating under a compressive stress of 100 MPa in the z direction.

The three empirical test cases were simulated with good accuracy by the FBG_SiMul software, as shown in Fig. 4 and Table 1. Thus, it can be concluded that the software can represent the FBG response for different type of strain/stress fields.

5. Illustrative example

In this section, FBG_SiMul was used to simulate and design a delamination/crack monitoring solution based on FBG sensors. A double cantilever beam (DCB) FEM model, based on the work presented by Pereira et al. in [3], was used to represent the delamination phenomenon. The complete description

Table 1

Software empirical validation: comparison between theoretical and FBG_SiMul simulation for the three known cases.

Test cases	(nm)	Theoretical results	FBG_SiMul simulation
Uniform strain	$\Delta\lambda$	12.16	12.16
	$\Delta\lambda_{WV}$	0	0
Non-uniform strain	$\Delta\lambda$	9.15	9.14
	$\Delta\lambda_{WV}$	6.07	6.08
Transverse stress	$\Delta\lambda$	0	0
	$\Delta\lambda_{WV}$	0.38	0.38

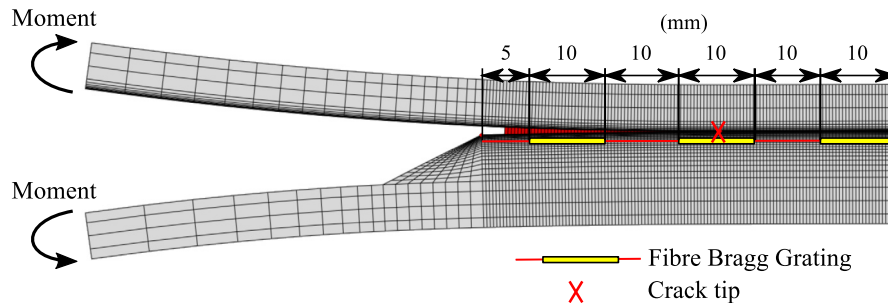


Fig. 5. Virtual FBG array configuration in the DCB specimen.

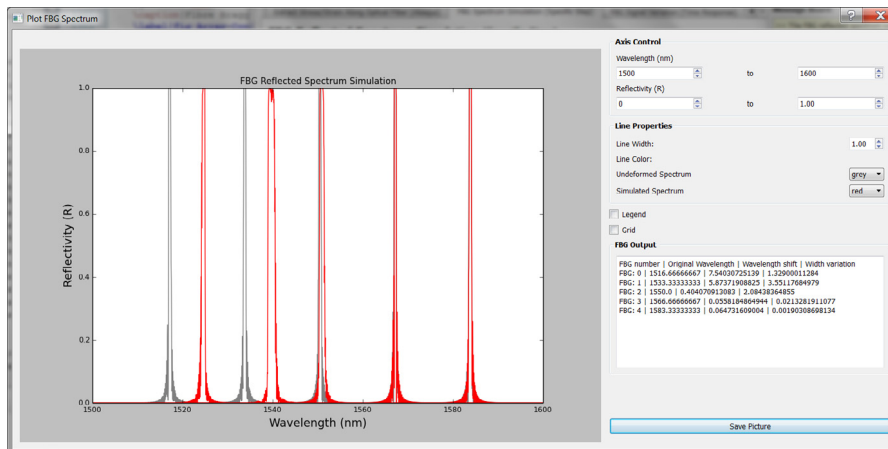


Fig. 6. FBG_SiMul plot window: FBG reflected spectrum simulation for the non-uniform strain contribution. The five peaks are the reflected spectrum of the five FBG sensors, where the grey curves represent the unstrained state and the red curves the deformed state. (For interpretation of the references to colour in this figure legend, the reader is referred to the web version of this article.)

of the FEM model and the simulation tutorial can be found in the FBG_SiMul user-manual.

The simulated virtual FBG array was composed of 5 gratings, spaced by 10 mm (see Fig. 5), and its path was a 0.03 mm, line parallel with the delamination plane. The FBG array spectrum response in the presence of a crack was simulated using the FBG_SiMul tab 3; and, the FBG signal response during the delamination process was simulated using the FBG_SiMul tab 4.

5.1. FBG spectrum simulation

The reflected spectrum was simulated when the crack tip was situated 36 mm from the beginning of the optical fibre line, meaning that the crack tip was located at middle of the second grating.

A screenshot of the FBG_SiMul plot/output window is shown in Fig. 6, where the deformed reflected spectrum (red curves) can be compared with the original reflected spectrum (grey curves). It can be observed that the two first FBGs measure a high amount of wavelength shift ($\Delta\lambda$) and peak width variation ($\Delta\lambda_{WV}$), used by the presence of the crack.

5.2. FBG time response simulation

The FBG sensor response during delamination of the DCB specimen (from an undamaged to a full damage state) was simulated using the tab 4-FBG Signal Variation. A screenshot of the FBG_SiMul plot/output window is shown in Fig. 7, where the top plot represents the wavelength shift ($\Delta\lambda_{WV}$), and the bottom plot represents the peak width variation ($\Delta\lambda$). This

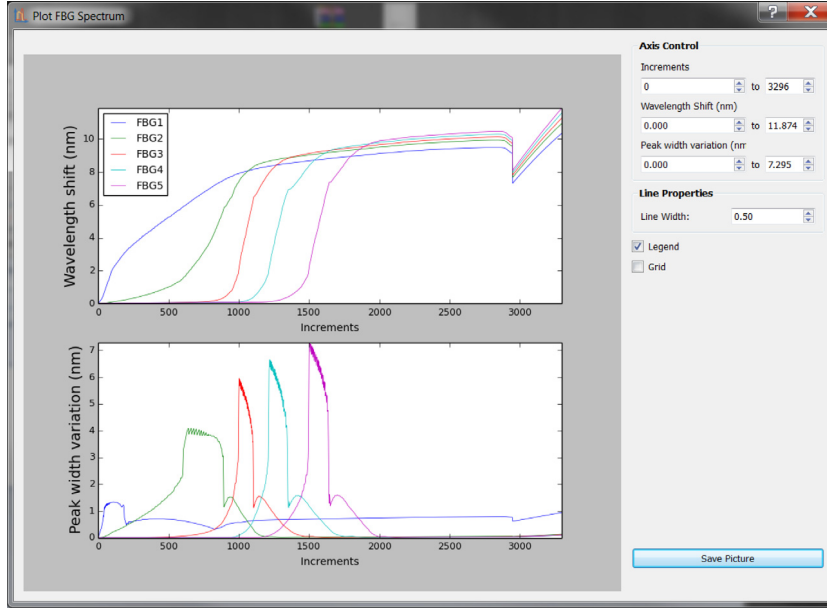


Fig. 7. FBG.SiMul plot window: FBG time response simulation.

simulation shows an increase of the $\Delta\lambda$ as the crack passes the position of the grating, caused by change in the material compliance and load distribution; and, an increase of the $\Delta\lambda_{WV}$ when the crack is near the grating, caused by a non-uniform strain field generated at the crack tip.

6. Conclusions

FBG.SiMul provides the user with a tool to study and design structural health monitoring solutions based on FBG sensors. The software is divided into 3 main functionalities: a tool to extract the stress and strain along an optical fibre path from a FEM model; a tool to simulate the reflected spectrum for a specific time increment; and a tool to simulate the FBG time response.

The software uses a modified version of the *T*-Matrix method to simulate the FBG signal from a FEM model. Thus, it can simulate the FBG response independently of the type of structure, loading or application. Also, the software removes the need for a fibre optic expert to plan and design FBG monitoring solutions. The user interacts with the software through a user-interface, meaning that no programming knowledge is required, making parameter manipulation more intuitive and fast. Also, the input data is pre-checked by the software, meaning that the simulation is robust and does not crash.

Acknowledgement

The author acknowledges the Seventh Framework Programme (FP7) for funding the project MareWint (Project reference: 309395) as Marie-Curie Initial Training Network.

Appendix A. Spectrum simulation theory

In a free state, without strain and at a constant temperature, the spectral response of a homogeneous FBG is a single peak

centred at wavelength λ_b , which can be described by the Bragg condition [3], as shown in Eq. (1).

$$\lambda_b = 2n_{\text{eff}}\Lambda_0. \quad (1)$$

The parameter n_{eff} is the mean effective refractive index at the location of the grating, Λ_0 is the constant nominal period of the refractive index modulation, and the index 0 denotes unstrained conditions (initial state).

The change in the grating period due to a uniform strain field is described in Eq. (2),

$$\Lambda(x) = \Lambda_0[1 + (1 - p_e)\varepsilon_{\text{FBG}}(x)] \quad (2)$$

where the parameter p_e is the photo-elastic coefficient, and $\varepsilon_{\text{FBG}}(x)$ is the strain variation along the optical fibre direction [7]. The variation of the index of refraction δn_{eff} of the optical fibre is described by Eq. (3),

$$\delta n_{\text{eff}}(x) = \overline{\delta n_{\text{eff}}} \left\{ 1 + v \cos \left[\frac{2\pi}{\Lambda_0} x + \phi(x) \right] \right\} \quad (3)$$

where v is the fringe visibility, $\phi(x)$ is the change in the grating period along the length, and $\overline{\delta n_{\text{eff}}}$ is the mean induced change in the refractive index [7].

By the couple-mode theory, the first order differential equations describing the propagation mode through the grating x direction are given by Eqs. (4) and (5).

$$\frac{dR(x)}{dx} = i\hat{\sigma}R(x) + i\kappa S(x) \quad (4)$$

$$\frac{dS(x)}{dx} = i\hat{\sigma}S(x) + i\kappa R(x). \quad (5)$$

The parameter $R(x)$ and $S(x)$ are the amplitudes of the forward and backward propagation modes, respectively, $\hat{\sigma}$ is the self-coupling coefficient as function of the propagation wavelength λ , and κ is the coupling coefficient between the two propagation modes [7–9]. The self-coupling coefficient $\hat{\sigma}$ for

a uniform grating ($\phi(x) = 0$) in function of the propagation wavelength λ is described in Eq. (6), where the parameter λ_b is the FBG reflected wavelength in an unstrained state defined by the Eq. (1).

$$\hat{\sigma} = 2\pi n_{\text{eff}} \left(\frac{1}{\lambda} - \frac{1}{\lambda_b} \right) + \frac{2\pi}{\lambda} \overline{\delta n_{\text{eff}}} \quad (6)$$

The coupling coefficient between the two propagation modes κ is defined by Eq. (7), where the parameter m is the striate visibility that is ≈ 1 for the conventional single mode FBG [8,9].

$$\kappa = \frac{\pi}{\lambda} m \overline{\delta n_{\text{eff}}} \quad (7)$$

Spectrum reconstruction

The optical response matrix of the i th (each FBG segment) uniform grating can be described by the coupled mode theory [4,8]. By considering the FBG length (L) divided in n short segments, then the $\Delta x = L/n$ is the length of each segment. Note that n is constrained by the grating period [8], as described by Eq. (8).

$$n \leq \frac{2n_{\text{eff}}}{\lambda_b} L \quad (8)$$

For the FBG length limits, $-L/2 \leq x \leq L/2$, and the boundary conditions, $R(-L/2) = 1$ and $S(L/2) = 0$, the solution of the coupling mode of Eqs. (4) and (5) can be expressed as:

$$\begin{bmatrix} R(x_{i+1}) \\ S(x_{i+1}) \end{bmatrix} = F_{x_i, x_{i+1}} \begin{bmatrix} R(x_i) \\ S(x_i) \end{bmatrix} \quad (9)$$

where $R(x_i)$ and $S(x_i)$ are the input light wave travelling in the positive and negative directions, respectively, and $R(x_{i+1})$ and $S(x_{i+1})$ are the output waves in the positive and negative directions, respectively. Thus, the transfer-matrix $F_{x_i, x_{i+1}}$ for each segment (Δx) of the grating can be calculated using the Eqs. (10) and (11).

$$F_{x_i, x_{i+1}} = \begin{bmatrix} S_{11} & S_{12} \\ S_{21} & S_{22} \end{bmatrix} \quad (10)$$

$$\begin{cases} S_{11} = \cosh(\gamma_B \Delta x) - i \frac{\hat{\sigma}}{\gamma_B} \sinh(\gamma_B \Delta x) \\ S_{12} = -i \frac{\kappa}{\gamma_B} \sinh(\gamma_B \Delta x) \\ S_{21} = i \frac{\kappa}{\gamma_B} \sinh(\gamma_B \Delta x) \\ S_{22} = \cosh(\gamma_B \Delta x) + i \frac{\hat{\sigma}}{\gamma_B} \sinh(\gamma_B \Delta x) \\ \gamma_B = \sqrt{\kappa^2 - \hat{\sigma}^2} \end{cases} \quad (11)$$

Finally, the grating total response matrix F is obtained by multiplication of each segment response matrix, as described in Eq. (12).

$$F = F_{x1} \cdot F_{x2} \dots F_{xn} \quad (12)$$

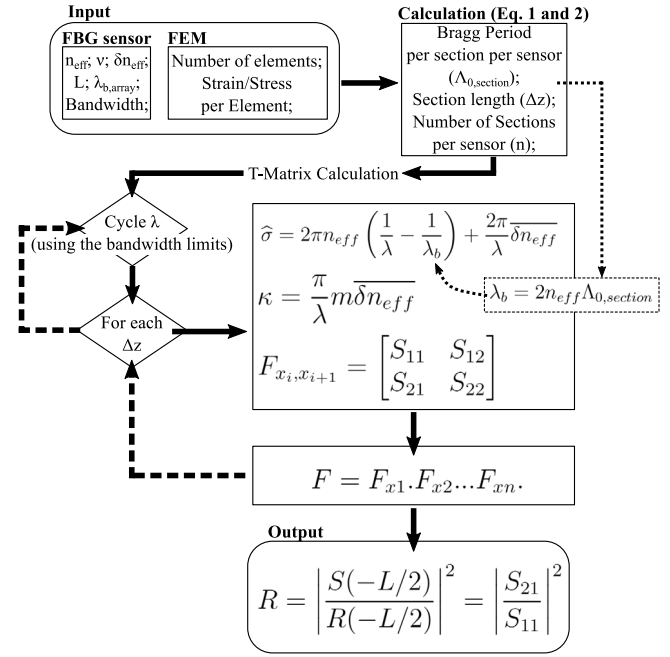


Fig. 8. FBG_SiMul spectrum simulation algorithm structure.

And, the reflectance of the grating can be described by the Eq. (13).

$$R = \left| \frac{S(-L/2)}{R(-L/2)} \right|^2 = \left| \frac{S_{21}}{S_{11}} \right|^2 \quad (13)$$

Appendix B. FBG_SiMul spectrum simulation algorithm structure

The structure of the spectrum simulation algorithm implemented in the FBG_SiMul is shown in Fig. 8.

References

- [1] Braga DFO, Tavares SMO, da Silva LFM, Moreira PMGP, de Castro PMST. Advanced design for lightweight structures: Review and prospects. *Prog Aerosp Sci* 2014;69:29–39. <http://dx.doi.org/10.1016/j.paerosci.2014.03.003>.
- [2] Takoutsing P, Wamkeue R, Ouhrouche M, Slaoui-Hasnaoui F, Tameghe T, Ekemb G. Wind Turbine Condition Monitoring: State-of-the-Art Review, New Trends, and Future Challenges. *Energies* 2014;7: 2595–630. <http://dx.doi.org/10.3390/en7042595>.
- [3] Pereira GF, Mikkelsen LP, McGugan M. Crack detection in fibre reinforced plastic structures using embedded fibre Bragg grating sensors: Theory, model development and experimental validation. *PLoS One* 2015; 10:e0141495. <http://dx.doi.org/10.1371/journal.pone.0141495>.
- [4] Hu H, Li S, Wang J, Wang Y, Zu L. FBG-based real-time evaluation of transverse cracking in cross-ply laminates. *Compos Struct* 2016;138: 151–60. <http://dx.doi.org/10.1016/j.compstruct.2015.11.037>.
- [5] Hassoun O, Tarfoui M, El Malk A. Numerical simulation of fiber Bragg grating spectrum for mode-delamination detection. *Int J Mech Aerosp, Ind Mechatronics Eng* 2015;9:144–9.
- [6] Yamada M, Sakuda K. Analysis of almost-periodic distributed feedback slab waveguides via a fundamental matrix approach. *Appl Opt* 1987;26: 3474–8. <http://dx.doi.org/10.1364/AO.26.003474>.
- [7] Peters K, Studer M, Botsis J, Iocco A, Limberger H, Salathé R. Embedded optical fiber Bragg grating sensor in a nonuniform strain field: Measurements and simulations. *Exp Mech* 2001;41:19–28. <http://dx.doi.org/10.1007/BF02323100>.

- [8] Ling H-Y, Lau K-T, Jin W, Chan K-C. Characterization of dynamic strain measurement using reflection spectrum from a fiber Bragg grating. *Opt Commun* 2007;270:25–30. <http://dx.doi.org/10.1016/j.optcom.2006.08.032>.
- [9] Chen Y, Li J, Yang Y, Chen M, Li J, Luo H. Numerical modeling and design of mid-infrared FBG with high reflectivity. *Opt Int J Light Electron Opt* 2013;124:2565–8. <http://dx.doi.org/10.1016/j.ijleo.2012.07.016>.
- [10] Ikhlef A, Hedara R, Chikh-bled M. Uniform fiber Bragg grating modeling and simulation used matrix transfer method. *IJCSI Int J Comput Sci* 2012; 9:368–74.
- [11] Bjerkan L, Johannessen K, Guo X. Measurements of Bragg grating birefringence due to transverse compressive forces. In: *Proc. 12th International Conference on Optical Fiber Sensors*, Vol. 16. 1997. p. 60–3.
- [12] Jülich F, Roths J. In: Berghmans F, Mignani AG, van Hoof CA, editors. comparison of transverse load sensitivities of fibre bragg gratings in different types of optical fibres. *Opt Sens Detect*, 2010. p. 77261N. <http://dx.doi.org/10.1117/12.854019>.
- [13] Sorensen L, Botsis J, Gmür T, Cugnoni J. Delamination detection and characterisation of bridging tractions using long FBG optical sensors. *Compos Part A Appl Sci Manuf* 2007;38:2087–96. <http://dx.doi.org/10.1016/j.compositesa.2007.07.009>.
- [14] Stutz S, Cugnoni J, Botsis J. Crack – fiber sensor interaction and characterization of the bridging tractions in mode I delamination. *Eng Fract Mech* 2011;78:890–900. <http://dx.doi.org/10.1016/j.engfracmech.2011.01.014>.